Structural properties of amorphous hydrogenated carbon. III. NMR investigations

C. Jäger,* J. Gottwald, and H. W. Spiess
Max-Planck-Institut für Polymerforschung, Postfach 3148, D-55021 Mainz, Germany

R. J. Newport
Physics Laboratory, The University, Canterbury, Kent CT2 7NR, United Kingdom
(Received 27 September 1993)

Our NMR studies give experimental evidence of bonding heterogeneity in samples of *a*-C:H on the nanometer scale. Two classes of protons were identified with distinctly different spin-lattice-relaxation behavior. The difference in the spin-lattice relaxation provides a means of spectral editing of cross-polarization magic-angle spinning, combined rotation and multiple-pulse spectroscopy, dipolar dephasing spectra, and multiple quantum NMR experiments. This combination of the various NMR techniques allows for a detailed structural investigation of *a*-C:H, e.g., the sp^2:sp^3 ratio, the relative amount of hydrogenated and nonhydrogenated carbons, etc. A model incorporating the heterogeneity is established and discussed. The NMR results are compared with neutron spectroscopy and diffraction data.

I. INTRODUCTION

In this paper we report the results of various NMR measurements performed on the same samples used in the high-resolution neutron-diffraction studies and the inelastic neutron-scattering experiments (see papers I and II,[1,2]). This enables a direct comparison of the results obtained by different techniques and allows for a more detailed interpretation of the data.

The major results of the neutron-scattering and diffraction experiments[1,2] can be summarized as follows: (1) The neutron-diffraction experiments indicate that the single:double bonds exist in a ratio of approximately 2.7:1 up to 3.6:1 and (2) most of the sp^2 carbon is in the olefinic and not in the aromatic/graphitic form. There was also evidence for a small amount of molecular hydrogen.

Additionally, the inelastic neutron-scattering data have been used to provide quantitative estimates of the concentration of CH_x species. The new assignments have been used to show that the dominant contributions to the high-frequency (>500 cm^{-1}) region were attributed to carbon moieties in the form of sp^3 CH_2 and CH groups, with at least as many CH_2 as CH groups, but few ($<10\%$) CH_3 groups.

Among the numerous techniques used for studying the structure of such materials, NMR is becoming increasingly important. Several papers have previously reported results from ^{13}C magic-angle spinning (MAS) NMR experiments with cross-polarization (CP) and proton dipolar decoupling measurements on systems with a high hydrogen content.[3–6] The resulting ^{13}C CP/MAS spectra normally consist of two broad resonances. One resonance at approximately 50 ppm (relative to TMS) is assigned to sp^3 hybridized carbons, and the other resonance at about 130 ppm is assigned to sp^2 carbon. One can also identify and quantify hydrogenated and nonhydrogenated carbons in *a*-C:H by gated decoupling experiments.[5–7]

In a previous communication[8] we have suggested the existence of structural heterogeneity on a nanometer scale in our *a*-C:H samples by exploiting the multicomponent ^{1}H spin-lattice-relaxation behavior. Two distinct types of protons clusters (here "proton cluster" is taken to mean a group of hydrogen atoms exhibiting the same relaxation behavior, spatially separated from the other proton clusters in the sample) can be distinguished this way. A simple model has been proposed consisting of protons distributed in the sp^2-sp^3 carbon network and short chains of CH_2 and CH groups separated by a "layer" of nonprotonated sp^2 carbons.

In the following we will give more evidence and quantitative results on this structural heterogeneity using various NMR techniques. The standard CP/MAS experiments with and without dipolar dephasing yield quantitative information about the hybridization and the relative amount of hydrogenated and nonhydrogenated carbons. High-resolution combined rotation and multiple-pulse spectroscopy[9,10] (^{1}H-CRAMPS) experiments have been used to characterize the proton species (e.g., Ref. 6), whereas multiple quantum NMR (Refs. 11–13) is a suitable tool to characterize the distribution of protons. For clustered distributions it is possible to determine the cluster size, i.e., the average number of interacting protons. Recent applications, for example, dealt with the determination of the cluster sizes in hydrogenated silicon and silicon carbide and adsorbed hexamethylbenzene in a zeolite.[14–17]

II. EXPERIMENTAL DETAILS

A. Samples

Two samples of *a*-C:H were prepared using a saddle-field fast-atom source (see explicit description in Ref. 1) using acetylene and propane as precursor gases for the samples, respectively. The deposition conditions (effective beam energy: 960 eV, system pressure: 1.4×10^{-4} mbar) yield hard forms of the *a*-C:H samples. The sample densities (1.8 and 2.0 g/cm^3 for the two sam-

ples) were determined using a residual volume technique and the compositions were obtained from Carlo-Erba CHN combustion analyses. The acetylene prepared sample has a hydrogen content of 35 at. %, the other of 32 at. %.

B. NMR techniques

All NMR measurements have been carried out using a Bruker MSL 300 spectrometer at a ^{13}C resonance frequency of 75.47 MHz and a ^{1}H frequency of 300.13 MHz. The high-resolution ^{13}C spectra have been measured with cross polarization (CP), magic-angle sample spinning (MAS) and dipolar decoupling (DD).[9] Spectra were also recorded using the TOSS (total suppression of sidebands) pulse sequence[10] that removes rotational sidebands arising from inhomogeneous interactions larger than the spinning frequency. In order to spectrally edit the high-resolution ^{13}C spectra, the proton magnetization is inverted by a π pulse followed by a fixed inversion recovery delay [see Fig. 1(a)]. Because we can distinguish two differently relaxing (T_1) proton systems in our samples, we can suppress the magnetization of one system by setting the inversion recovery delay to the time when one of the proton magnetization passes through zero while relaxing to the equilibrium magnetization M_0. Then the remaining proton magnetization of the order system can be used, e.g., for the polarization transfer in CP. Thus, the ^{13}C chemical shifts can be determined and correlated to those protons that have been exploited for the CP process.

Also, the gated dipolar decoupling experiment[18] allows one to distinguish between hydrogenated and nonhydrogenated carbons by switching off the dipolar decoupling for a short time. The magnetization of protonated carbons disappears within approximately 60 μs because of the strong heteronuclear dipolar coupling (dipolar dephasing). $^{13}CP/TOSS$ experiments can advantageously be used for these gated decoupling experiments,[19] because the data acquistion will always start at the echo maximum. Thus, proper phasing of the spectra is ensured. For this experiment the decoupler is switched off between two of the ^{13}C π pulses of the TOSS sequence [see Fig. 1(a)]. As explained before, an inversion of the proton magnetization allows the study of the dipolar dephasing for the various carbon resonances independently. Typical ^{1}H and ^{13}C $\pi/2$ pulse lengths were 4 μs. The MAS spinning frequency was 3.1 kHz. This ensures a sufficient suppression of spinning sidebands for the CP/MAS experiments and enables gated decoupling times of up to 300 μs using the TOSS sequence. The cross-polarization time was 1 ms, the repetition time was 1–2 s and typically between 1000 and 2000 scans were averaged per spectrum. For our samples, the inversion recovery delays used for selecting the two different proton clusters were 8 and 35 ms. Furthermore, ^{13}C single-pulse excitation has been used for the correct determination of the sp^2:sp^3 ratio with repetition times of 10 s.

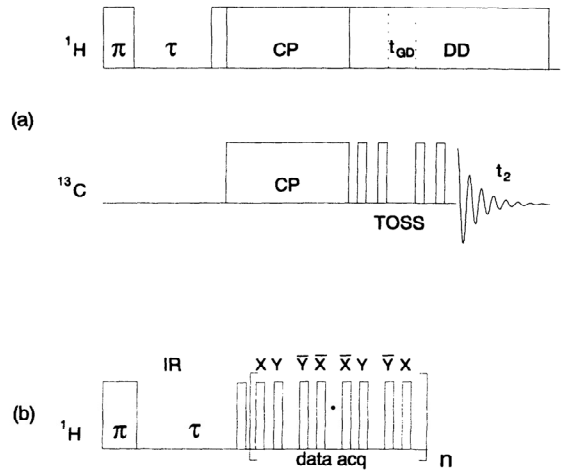

FIG. 1. Pulse sequences used for the spectral editing of both ^{13}C NMR (a) and high-resolution ^{1}H NMR (b). In both cases the ^{1}H magnetization is inverted by a π pulse. After a suitably chosen delay τ the normal CP experiment follows. For determining the ratio of hydrogenated and nonhydrogenated carbons the dipolar decoupling (DD) is switched off for a short time t_{GD} between two of the TOSS π pulses. In case of the ^{1}H NMR the multiple-pulse sequence MREV 8 has been used.

High-resolution ^{1}H NMR spectra have been acquired using multiple-pulse sequences (MREV 8 in this case) combined with MAS [referred to as CRAMPS (Ref. 10)] for identifying the proton species. The schematic pulse sequence preceding inversion of the magnetization is shown in Fig. 1(b). For these experiments a special Bruker CRAMPS probe has been used. The MAS frequency was 1.8–2.0 kHz; the $\pi/2$ pulse length was 2 μs. ^{1}H and ^{13}C chemical shifts are referenced to tetramethylsilane (TMS).

The basic idea of multiple quantum (MQ) NMR experiments in solids is to exploit the homonuclear dipolar coupling between the nuclear spins. This can be used to investigate the number of correlated spins. The schematic pulse sequence of a MQ NMR experiment is shown in Fig. 2. Theoretical details of the experiments can be found in the comprehensive reviews.[11,12] The experiment consists of three periods: preparation, mixing, and detection. During the preparation period an eight-pulse sequence irradiates the spin system. The average Hamiltonian developed by this cycle is

$$\mathbf{H}^{(0)} = -\frac{1}{2}\sum_{j<k} D_{jk}(\mathbf{I}_j^{+}\mathbf{I}_k^{+} + \mathbf{I}_j^{-}\mathbf{I}_k^{-}) \tag{1}$$

and creates even-order MQ coherences 0, ± 2, ± 4, $\pm 6, \ldots, \pm 2n$. The mixing period is similar to the preparation period except that each pulse phase is shifted by 90°, creating the same average Hamiltonian but with negative sign. Thus the unobservable MQ coherences (developed during the preparation period) are converted back into observable populations as at the beginning of the preparation period. Then the magnetization is read out by a pulsed spin locking sequence after a short delay of approximately 1 ms to allow dephasing of spurious unwanted coherences. This signal is stored as the first point of a MQ signal. Hence, the entire sequence is repeated n times by advancing the overall pulse phase Φ of the preparation sequence by $\Delta\Phi$. This ensures separation

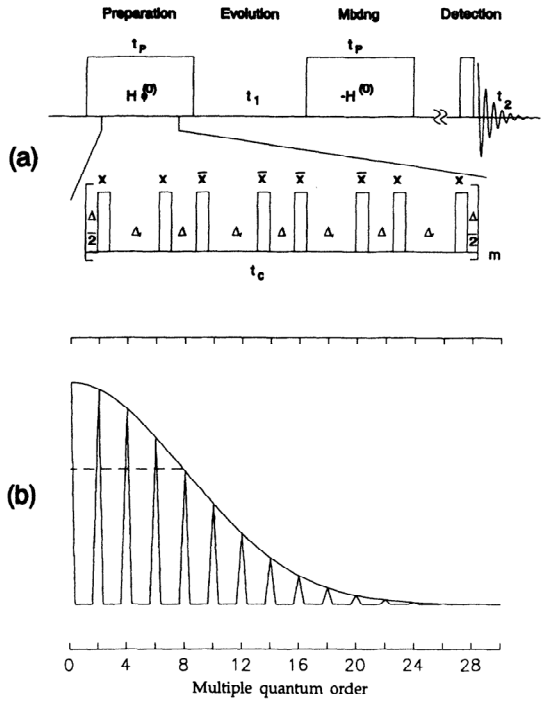

FIG. 2. Schematic picture of the multiple quantum experiment (a) and the basic shape of a MQ spectrum (b). For details see text.

of the MQ coherences in the MQ spectrum. Typically 60 increments have been used allowing the recording of MQ orders up to 30 ($\Delta\Phi = 6°$). The $\pi/2$ pulsewidth was 2.8 μs which results in a cycle time of $t_c = 67$ μs for the eight-pulse sequence. Figure 2(b) shows a theoretical MQ spectrum, obtained after Fourier transformation. Combinatorial arguments predict that the intensity of the nth-order coherence, $I(n)$, in an isolated cluster of N_c spins can be approximated by a Gaussian distribution ($N \geq 6$):

$$I(n) \propto \exp(-n^2/N_c) \; . \tag{2}$$

Consequently, the number of correlated spins N_c can be determined by fitting the amplitudes of the MQ coherences to a Gaussian line. Varying the preparation period in multiples of the basic eight-pulse preparation sequence, N_c can be determined as function of that time, which in turn allows the discrimination between a limited cluster size or a continuous distribution. In the first case the number of correlated spins N_c remains constant after a sufficiently long preparation time.

III. RESULTS AND DISCUSSION

In the following we will discuss the experimental results obtained for the acetylene prepared sample in detail. Within the signal-to-noise ratio the results of the NMR measurements of the sample with propane as precursor gas are almost identical to the acetylene prepared a-C:H sample.

In our previous paper we reported a two-component ^{1}H spin-lattice relaxation in our samples of a-C:H. This two-component behavior is due to two differently fast relaxing proton spin systems. In particular this two-component behavior has nothing to do with nonexponential spin-lattice relaxation as often found in disordered solids. Such nonexponential behavior can, in principle, be possible also in our case; however our ^{1}H inversion recovery curves suggest exponential relaxation for the two differently relaxing proton systems within the signal-to-noise ratio. Assuming a biexponential relaxation behavior we obtain two time constants of 14 and about 120 ms.[8] These curves are shown in Fig. 3 on top. The most relevant point is that no equilibrium of the spin-lattice relaxation occurs on a time scale up to about 100 ms between the two proton reservoirs. Obviously, this implies that proton spin diffusion between the two differently relaxing proton systems is not relevant; hence our conclusion of a "layer" of nonhydrogenated sp^2 carbons separating the two proton clusters (Ref. 8 and Fig. 8 here).

Figure 3 summarizes the results of the ^{1}H T_1 spectral editing of the ^{13}C CP/MAS spectra. If a long recovery delay of 200 ms or longer is chosen, the normal CP spectrum is observed [Fig. 3(a)]. The spectrum clearly shows sp^2 carbons at 130 ppm and a broad resonance due to sp^3 carbons at 65 ppm (peak position). These results are similar to those of other authors.[3,5–7] However, if the

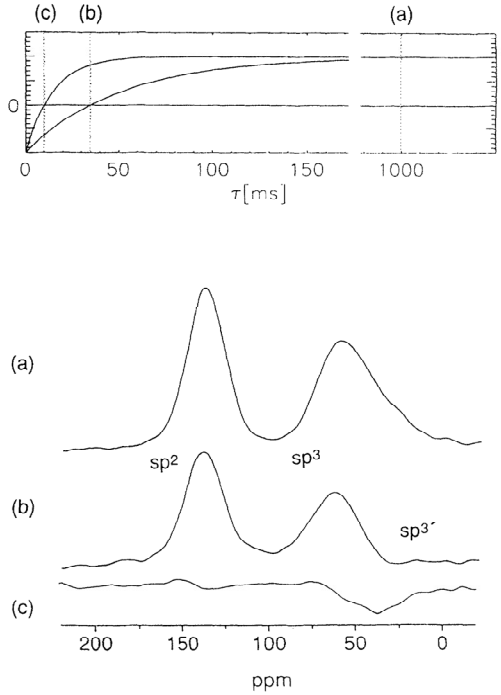

FIG. 3. ^{13}C CP spectra as function of the delay τ between the π pulse and the beginning of the ordinary CP experiment. Case (a): Normal spectrum showing sp^2 and sp^3 resonances as usual. Case (b): Fast relaxing protons were used for the cross polarization. sp^2 and sp^3 signals are found. Case (c): Slowly relaxing protons cross polarize only $sp^{3'}$ carbons. For further details see text.

recovery delay is set to 35 ms then the fast relaxing protons are selected for the cross-polarization transfer to the carbons. For this inversion recovery delay no ^{1}H magnetization of the slower relaxing protons is available, since their net magnetization is zero. Under this condition strong ^{13}C resonances due to sp^2 and sp^3 carbons are observed [Fig. 3(b)]. Now, the peak position for the sp^3 resonance is still at 65 ppm, but the shoulder on the right-hand side of this line disappears [compare with Fig. 3(a)]. This can easily be explained by selecting 8 ms for the recovery delay. Now the proton magnetization of the slowly relaxing protons is exploited for the cross-polarization transfer. As can be seen from Fig. 3(c), the NMR signal is then negative as to be expected. More interesting is the fact, that those slowly relaxing protons cross polarize only sp^3 carbons (assigned as $sp^{3'}$ in the following) with a mean chemical shift of approximately 40 ppm which is distinctly different from the other sp^3 carbons. Additionally, this ^{13}C signal corresponds to that which disappears when selecting the fast relaxing protons [Fig. 3(b)]. Hence, the overall line shape [Fig. 3(a)] is simply the superposition of the two T_1 edited lineshapes [Figs. 3(b) and 3(c)]. A line deconvolution gives a $sp^{3'}$:sp^3 ratio of approximately 1:2.

Of course, single-pulse ^{13}C experiments without CP but with TOSS and decoupling have been carried out to determine the correct sp^2:sp^3 ratio. As reported in Ref. 6 there is no significant difference between the CP and single-pulse spectra. In our case, the sp^2 signal loss due to the TOSS sequence was corrected using the two-dimensional MAS sideband separation technique,[21] which does not require any guesses on the anisotropy of the various ^{13}C resonances. A correction factor of 1.55 was found for the sp^2 intensity which results in a sp^2:sp^3 ratio of 1.44 or (59±2)%:(41±2)%. Our correction factor agrees well with that of 1.6 (Ref. 6) exploiting the spinning speed dependence of the TOSS intensity.[22] In both cases the same MAS frequency of 3.1 kHz and magnetic-field strength has been used.

As pointed out in the Introduction, gated decoupling experiments yield reliable information on the ratio of hydrogenated and nonhydrogenated carbons. The results of those experiments are summarized in Fig. 4 and Table I. Since we can edit the carbon spectrum by the differently relaxing protons, it is easy to obtain correct experimental results for each of the carbon resonances separately plotting the line intensities as function of the gated decoupling time t_{GD}. These gated decoupling curves are usually analyzed by the equation[20,6]

$$I(t)=I_p \exp\left[-\frac{t_{GD}^2}{2T_p^2}\right]+I_n \exp\left[-\frac{t_{GD}}{T_n}\right] \quad (3)$$

with t_{GD} being the length of the decoupling pause. I_p is the amplitude of the Gaussian-like decaying part which is associated with the protonated carbons, hence the subscript p. I_n is the measure for the nonhydrogenated carbons which are assumed to decay exponentially.

As mentioned previously, the fast relaxing protons cross polarize both sp^2 and sp^3 carbons. Our gated decoupling data imply that only 20% of the sp^2 carbons are hydrogenated [Fig. 4(a)], whereas the corresponding relative amount is 35% for the sp^3 carbons [Fig. 4(b)]. This result together with the experimental fact of a strong CP effect for both sp^2 and sp^3 carbons (see discussion of Fig. 1) suggests that the fast relaxing protons are obviously statistically distributed in the sp^2-sp^3 carbon network.

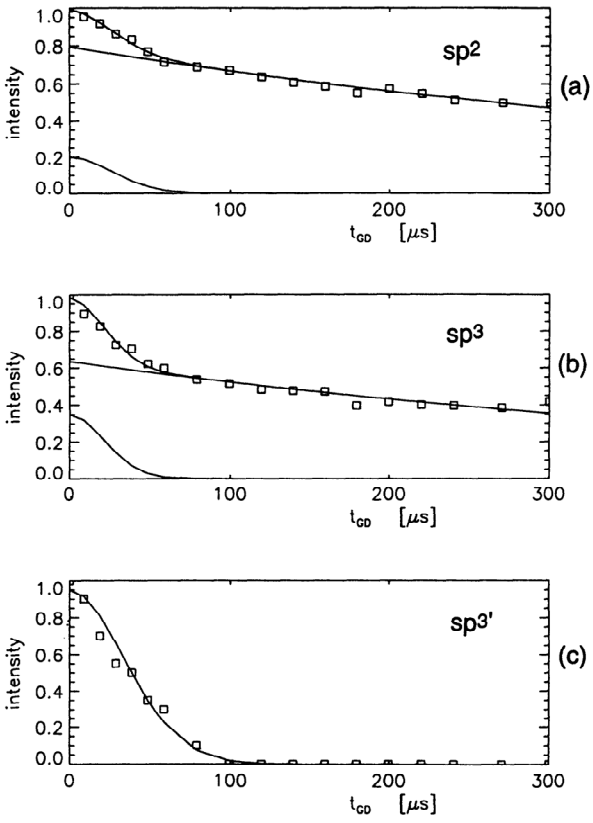

FIG. 4. Variation of the ^{13}C line intensities for the sp^2, sp^3, and $sp^{3'}$ resonances as function of the decoupling pause t_{GD}. Using Eq. (3) the relative amount of hydrogenated and nonhydrogenated carbon atoms is obtained. The results are listed in Table I.

TABLE I. Distribution of the carbons. The second column gives the relative amount of the carbons in the different hybridization states (sp^3 and $sp^{3'}$ are the carbons with the fast or slowly relaxing protons in the neighborhood, respectively). Columns 3 and 4 give the relative proportions (out of the numbers of column 2) for hydrogenated and nonhydrogenated carbons. High-resolution ^{1}H CRAMPS give a ratio of 1:1.44 for the fast and slowly relaxing protons which are attributed to sp^2 and sp^3 CH groups and $sp^{3'}$ CH_2 units, respectively.

	Rel. amount	Hydrogenated	Nonhydrogenated
sp^2	(59±2)%	20% (CH)	80%
sp^3	27%	35% (CH)	65%
	Total: (41±2)%		
$sp^{3'}$	14%	100% (CH_2)	

On the other hand, the $sp^{3'}$ carbons associated with the slower relaxing protons are fully hydrogenated within the S/N ratio [Fig. 4(c)]. This is important in so far as we have already mentioned the very small $sp^{3'}$ CP signal which arises from those protons. One straightforward conclusion is to assume those protons—and hence the associated carbons—to be confined to a small network region. One way of checking this assumption is to measure the high-resolution ^1H spectrum. These CRAMPS spectra are plotted in Fig. 5 in the usual way, where Fig. 5(a) shows again the complete spectrum and Figs. 5(b) and 5(c) represent the spectra obtained after T_1 editing with the two different inversion recovery delays as in the previous figures. The only difference to the former experiments is that the remaining proton magnetization is not transferred to the carbons but used to obtain the ^1H CRAMPS line shape. The overall spectrum shows a maximum at approximately 2 ppm with a shoulder at about 5–7 ppm and is quite similar to the spectra presented in Ref. 6. The whole pattern is inhomogeneously broadened by distributions of isotropic chemical shifts. Hence, it is impossible to deconvolute this NMR pattern, e.g., by two Gaussian lines as already mentioned in Ref. 6. However, this can easily be achieved by the spectral editing technique. The dotted lines in Fig. 5(a) show the result of such a procedure. Taking the area as a measure for the proton ratio we obtain a ratio of approximately 1:1.5 for the fast and slowly relaxing proton species, respectively.

Cross checking this quantitative result with the ^{13}C CP measurements (especially the different CP efficiencies) and taking into account the mean ^1H chemical shifts, the slowly relaxing protons are assumed to form sp^3 CH_2 groups which can form sections of polymerlike chains. Obviously these "chains" are short and confined to small regions in the network. Under these circumstances the CP effect is limited to the carbon of those CH_2 chain units which explains the small sp^3 carbon signal.

In contrast to this the fast relaxing protons are assumed to exist in sp^2 and sp^3 CH groups and these protons are statistically distributed. This ensures the strong cross-polarization effect when selecting this cluster, because one proton can cross polarize several carbons. This assignment is in good agreement with the inelastic neutron-scattering data suggesting approximately equal concentrations of sp^3 CH and CH_2 groups.[2] Following that assignment a CH:CH_2 ratio of about 60%:40% is obtained. The quantitative results are summarized in Table I.

The discussion so far has implied two conclusions. First, the fast relaxing protons are statistically distributed in the carbon network and secondly others should be confined to small network regions. This is a nearly perfect situation for multiple quantum NMR. Since we can

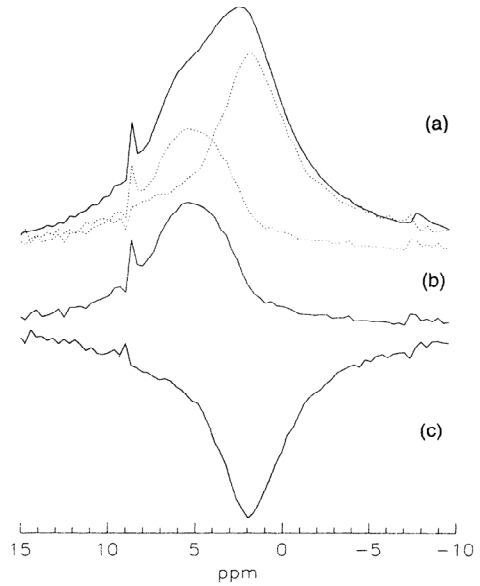

FIG. 5. Spectral editing of the high-resolution ^1H spectra (compare also Fig. 3). Case (a): Normal ^1H CRAMPS spectrum. Case (b): ^1H CRAMPS spectrum of the fast relaxing protons. Case (c): ^1H CRAMPS spectrum of the slowly relaxing protons. For further details see text.

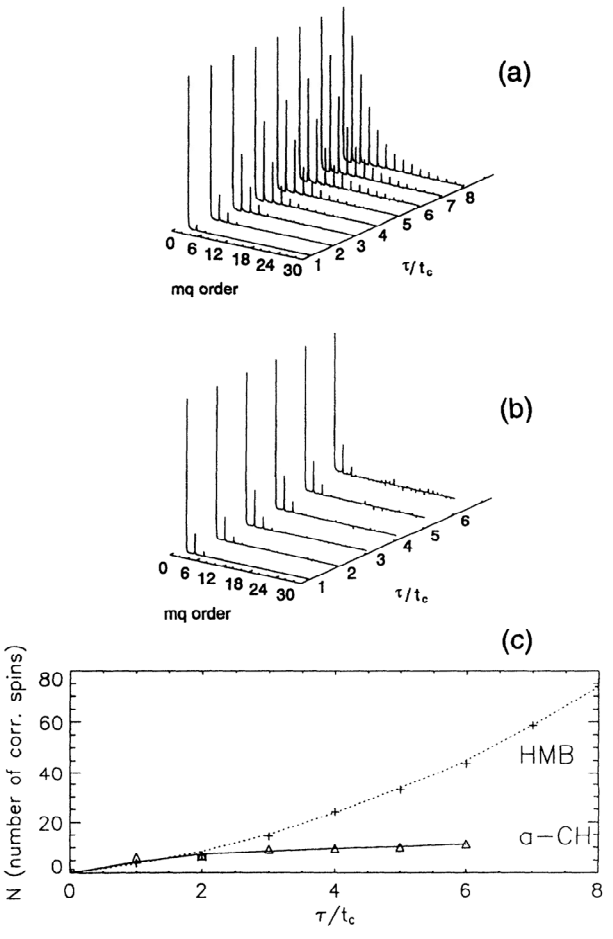

FIG. 6. Comparison of the MQ NMR spectra of hexamethylbenzene (a) and those of a-C:H (b). The number of correlated spins N_c as function of multiples of the preparation time cycle t_c are plotted in (c). Clearly in contrast to hexamethylbenzene there is a limited number of correlated spin for a-C:H.

select the two differently relaxing types of protons separately we can check experimentally whether those conclusions on the distributions of the protons are indeed true. Furthermore in case of a clustering of some protons, their size can be determined.

In Fig. 6 the MQ spectra of hexamethylbenzene [Fig. 6(a)] are compared with those of the *a*-C:H [Fig. 6(b)]. The number of correlated spins as function of the MQ preparation time is plotted and compared for the two samples in Fig. 6(c). Clearly, a continuous increase of the number of correlating spins N_c as function of the preparation time is found for hexamethylbenzene, as to be expected. But an obviously limited cluster size is found for the protons in *a*-C:H even if the MQ spectra of both types of protons are measured simultaneously. After a fast increase of N_c to about ten this number increases further only slowly.

For a correct interpretation of the MQ spectra of *a*-C:H, however, we have to perform those experiments for each of the proton clusters separately. The evolution of the MQ coherences for short preparation times are compared in Fig. 7 in the same way as in the other figures. The spectra and the graph of Fig. 7(b) clearly show a continuous increase of the number of correlated spins. These are the statistically distributed protons of the sp^2 and sp^3 CH groups. In contrast to it, the MQ spectra of the CH_2 groups do not change very much after the first preparation cycle. This means that even for the shortest preparation period (67 μs) all the spins are already correlated. According to Fig. 7(c) we have only about ten correlated protons which would result in a mean chain length of approximately five CH_2 units. This is clearly a heterogeneity on a nanometer scale.

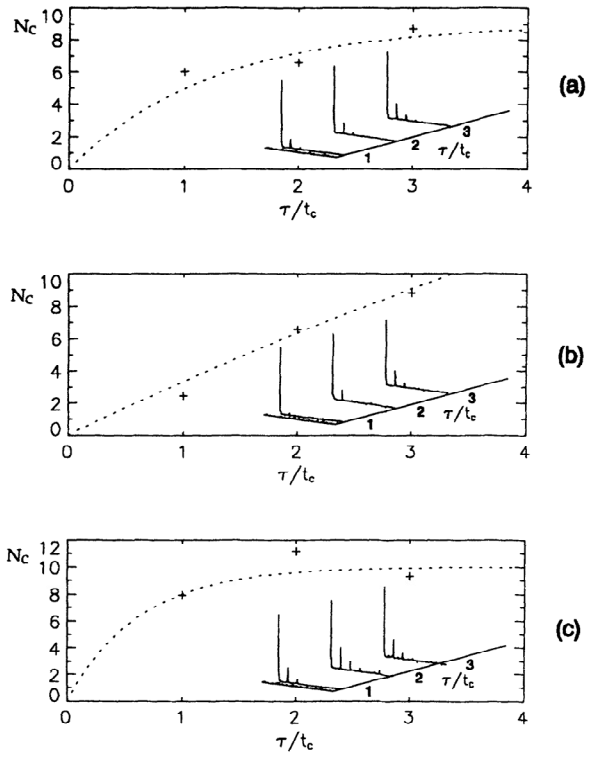

FIG. 7. Spectral editing of the MQ NMR spectra of *a*-C:H for the shortest preparation times. Case (a): Overall spectra and number of correlated spins N_c. Spectrum represents superposition of the signals due to the two differently relaxing proton "systems." Case (b): Fast relaxing protons are selected. The slow (almost linear increase of N_c suggests statistically distributed protons. Case (c): Slowly relaxation protons are chosen. Even after the shortest preparation time all spins are already correlated ($N_c = 10$).

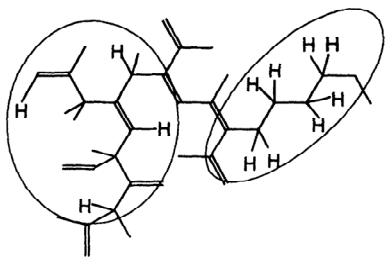

FIG. 8. Schematic model of the microstructure of *a*-C:H entirely based on the NMR data showing heterogeneity in the structure on a nanometer scale. For details see text.

All these NMR results can be summarized in a structural model which is schematically sketched in Fig. 8. It consists of short sections of CH_2 chains and statistically distributed CH groups in a sp^2-sp^3 carbon network with olefinic rather than aromatic carbons. These two environments are separated by regions of nonhydrogenated sp^2 carbons which are responsible for the breakdown of the ^1H spin diffusion which would otherwise equilibrate the spin-lattice-relaxation time. This microscopic model is entirely consistent with the quantitative results spatially averaged from neutron-diffraction and spectroscopy data presented in papers I and II.

IV. CONCLUSION

In the previous section the NMR results have been explained and discussed in terms of a model for the nanoheterogeneity in these *a*-C:H samples. One way of checking the consistency of these results is to calculate the hydrogen content using the numbers listed in Table I in conjunction with the structural model. Following this computation we obtain a hydrogen content of 33 at. %, in good agreement with the chemically determined composition of (35±1) at. % hydrogen. Because the neutron-scattering experiments[1,2] and these NMR measurements have been carried out using identical material it is instructive to compare the results of these complementary methods in more detail.

The neutron-scattering data give a $CH:CH_2$ ratio of about 1:1.25 ($\leq$20%). This agrees reasonably well with the ratio of 1:1.5 ($\leq$25%) found by the ^1H high-resolution NMR spectra. Furthermore, the hydrogen has a preference of bonding to sp^3 rather than to sp^2 carbons following the neutron-scattering data. This is supported by the NMR investigations where a ratio of 1:2 is obtained for sp^2 CH:sp^3 CH/CH_2 groups which results in a

ratio of 1:3 for the hydrogen atoms bound to sp^2 and sp^3 carbons, respectively.

There is, however, one discrepancy between the two sets of results. Whereas neutron scattering yields a ratio between single:double bonds in the range of 2.6:1 up to 3.7:1, the corresponding NMR value is about 4:1 ($\leq 10\%$). The reason for this discrepancy is not yet clear and requires further investigations.

Despite this difficulty of detail, the good coincidence between the NMR and the neutron-scattering data illustrates the high degree of complementary of the various data sets. This in its turn has allowed us to postulate in detail a model for the atomic-scale structure of *a*-C:H which differs significantly from those used hitherto.

ACKNOWLEDGMENTS

C.J. would like to thank the Deutsche Forschungsgemeinschaft for financial support. This work was also supported by the Deutsche Akademische Austauschdienst (DAAD) and the British Council within the Academic Research Collaboration Programme (ARC) and in the UK by the SERC. We would like to thank Dr. R. Lewis for his critical comments.

*Author to whom correspondence should be addressed.

[1]J. K. Walters, P. J. R. Honeybone, D. W. Huxley, and R. J. Newport, this issue, Phys. Rev. B **50**, 831 (1994).

[2]P. J. R. Honeybone, R. J. Newport, J. K. Walters, W. S. Howells, and J. Tomkinson, preceding paper, Phys. Rev. B **50**, 839 (1994).

[3]F. Jansen, M. Machonkin, S. Kaplan, and S. Hark, J. Vac. Sci. Technol. A **3**, 605 (1985).

[4]F. Kleber, K. Jung, H. Ehrhardt, I. Mühling, K. Breuer, H. Metz, and F. Engelke, Thin Solid Films **205**, 274 (1991).

[5]R. J. Gambogi, D. L. Cho, H. Yasuda, and F. D. Blum, J. Polym. Sci. Polym. Chem. Ed. **29**, 1801 (1991).

[6]U. Schwerk, F. Engelke, R. Kleber, and D. Michel, Thin Solid Films **230**, 102 (1993).

[7]K. R. Carduner, M. J. Rokosz, M. A. Tamor, and W. C. Vassell, Appl. Magn. Reson. **2**, 647 (1991).

[8]C. Jäger, J. J. Titman, and R. J. Newport, Thin Solid Films **227**, 3 (1993).

[9]M. Mehring, *Principles of High-Resolution NMR in Solids* (Springer-Verlag, Berlin, 1983).

[10]B. C. Gerstein and C. R. Dybowski, *Transient Techniques in NMR of Solids* (Academic, New York, 1985).

[11]M. Munowitz and A. Pines, Adv. Chem. Phys. **66**, 1 (1987).

[12]D. P. Weitekamp, Adv. Magn. Reson. **11**, 111 (1983).

[13]B. E. Scruggs and K. K. Gleason, J. Magn. Reson. **99**, 149 (1992).

[14]J. Baum, K. K. Gleason, A. Pines, A. N. Garroway, and J. A. Reimer, Phys. Rev. Lett. **56**, 1377 (1986).

[15]K. K. Gleason, M. A. Petrich, and J. A. Reimer, Phys. Rev. B **36**, 3259 (1987).

[16]M. A. Petrich, K. K. Gleason, and J. A. Reimer, Phys. Rev. B **36**, 9722 (1987).

[17]R. Ryoo, S. B. Liu, L. C. de Menorval, K. Takegoshi, B. F. Chmelka, M. Trecoske, and A. Pines, J. Chem. Phys. **91**, 6575 (1987).

[18]S. J. Opella and M. H. Frey, J. Am. Chem. Soc. **101**, 5854 (1979).

[19]J. Witt, D. Fenzke, and W. D. Hoffmann, Appl. Magn. Reson. **3**, 151 (1992).

[20]P. D. Murphy, T. J. Cassady, and B. C. Gerstein, Fuel **61**, 1233 (1982).

[21]S. Féaux de Lacroix, J. J. Titman, A. Hagemeyer, and H. W. Spiess, J. Magn. Reson. **97**, 435 (1992).

[22]F. Engelke, B. Maess, and D. Fenzke, J. Magn. Reson. **84**, 441 (1989).